



# Experimental investigation of jointed rock breaking under a disc cutter with different confining stresses

Qibin Lin<sup>a</sup>, Ping Cao<sup>a</sup>, Rihong Cao<sup>a,b,\*</sup>

<sup>a</sup> School of Resources and Safety Engineering, Central South University, Changsha, China

<sup>b</sup> School of Civil, Environmental and Mining Engineering, The University of Western Australia, Perth, Australia



## ARTICLE INFO

### Article history:

Received 9 March 2018

Accepted 26 June 2018

Available online 13 July 2018

### Keywords:

TBM disc cutter  
Jointed rock mass  
Confining stress  
Crack propagation  
Failure mode

## ABSTRACT

Extensive and detailed investigations have been made to better understand the rock-breaking mechanism of the tunnel boring machine (TBM) disc cutter, but the crack propagation and failure modes induced by the disc cutter when the confining stresses and joint characteristics vary have not been comprehensively investigated. To address this area of research, a triaxial testing machine (TRW-3000) is modified to investigate the effect of different confining stresses (0, 2.5, 5, 7.5 and 10 MPa) on the rock breaking of different joint angles (0°, 30°, 60°, and 90°) induced by the disc cutter. In this series of tests, the crack propagation and failure modes of the intact and jointed rock with different confining stresses are analysed. During the experiments, four different types of failure modes have been observed. The failure mode is affected by the joint orientation at low confining stress. The existence of joints has no obvious effect on the failure mode when the confining stress increases to a certain extent.

© 2018 Académie des sciences. Published by Elsevier Masson SAS. All rights reserved.

## 1. Introduction

Because of the high efficiency and safe operation, the tunnel boring machine (TBM) is widely utilised in large-scale infrastructure work, particularly tunnelling engineering [1]. However, in most excavation works, there are various types of discontinuities in the natural rock mass [2–5]. In addition, with the increase in excavation depths, the confining stress has been proven to be a crucial factor that affects the breaking efficiency during the TBM excavation [6–10]. Hence, the investigation of the rock-breaking mechanism under various geological conditions has important theoretical and practical significance. To date, many theoretical studies, laboratory tests, numerical simulations, and site observation investigations have been performed to separately investigate rock-breaking mechanisms such as the joint characteristic and confining stress. In theoretical studies, the scholars have introduced many rock-breaking models. The CSM model is one of the well-known prediction models in TBM tunnelling projects [11]. Based on laboratory tests, Bruland proposed the NTNU model, and the joint angle was considered to predict the penetration rate in this model [12]. Barton introduced the QTBM model with consideration of the joint angle [2].

Recently, many numerical simulation approaches have been widely used to study the rock fragmentation mechanism of the TBM cutter, including the finite element method (FEM), the displacement discontinuity method (DDM), and the distinct element method (DEM). For example, Liu et al. [13] analysed the effect of the confining stress on the TBM performance using

\* Corresponding author at: School of Resources and Safety Engineering, Central South University, Changsha, China.

E-mail address: 18229997417@163.com (R. Cao).

**Table 1**  
Basic mechanical parameters of the materials.

Rock-like material				Mica sheet			
Tensile strength (MPa)	Compressive strength (MPa)	Elastic modulus (GPa)	Poisson's ratio	Friction angle (°)	Cohesion (MPa)	Cohesion (MPa)	Friction angle (°)
2.75	22.95	22.70	0.23	49	1.16	0.01	10

the rock failure process analysis (RFPA). Marji et al. [14,15] applied the DDM to simulate crack propagation with disc cutters. Gong et al. [3] and Jiang et al. [4] used the DEM to examine the impact of the joint orientation on crack propagation during the indentation process of TBM cutters. Zhai et al. [5] used the General Particle Dynamics (GPD) to simulate the jointed rock failure process by disc cutters. These studies provide the action laws of the joint characteristic or confining stress on the rock-breaking process beneath disc cutters. However, the jointed rock-breaking process by a disc cutter under different confining stresses is notably complex, and there are assumptions in the simulation process, so the jointed rock-breaking mechanism between the cutter and the confining stress remains unclear.

Because of the theoretical difficulties and numerical simulation limitations, many experiments have been performed to investigate the rock-breaking mechanism under different confining stresses in intact rock mass. Innaurato et al. [6] performed indentation tests and found that the increase in confining stress was beneficial to the propagation of lateral cracks. The laboratory tests of Yin et al. indicate that rock breakages are restrained when the confining stress increases to some extent [16,17]. Liu and Wang [18] experimentally and numerically analysed the effect of the confining stress on the crack initiation and propagation. Entacher et al. [19] studied the rock failure process of a cutter, and observed that the median cracks were well developed at low confinement levels, but were restrained when the confining stress increased. The laboratory test by Chen and Labuz shows a similar crack propagation tendency, even for a sharp indenter [20]. Thus, crack propagation in intact rocks varies under different confining stress conditions.

Previous works provided important primary knowledge about the rock fragmentation mechanism of TBM cutters. However, in most of these studies, the effect of the joint characteristic and confining stress on the rock-breaking process under disc cutters was individually studied. During the excavation, the jointed rock mass is commonly under in situ stress conditions. Thus, it is of great importance to reveal the effect of the joint characteristic and confining stress on the rock-breaking process under the disc cutter. To systematically study the combined effect of the joint characteristic and confining stress, a series of laboratory tests were performed to analyse the crack propagation and failure modes of intact and jointed rocks for different confining stress values. In this work, the combined effect of the joint characteristic and confining stress on the cracking process of specimens is investigated, and the failure modes related to the cracking process are analysed. The effect of the joint orientation and confining stress is highlighted in this study.

## 2. Description of the experiments

### 2.1. Specimen preparation

Scholars have made different types of joints through natural rock and brittle rock materials, and studied the effect of joints on rock-breaking efficiency [21,22]. Apart from natural rocks, various materials have also been widely used by scholars, such as gypsum [23], concrete [24] and cement mortar [25–27]. For the samples made by cement mortar, because the main framework of the material is cement and sand, the cement is the adhesive material, and the sand can provide the frictional behaviour of the modelling material. This feature is similar to the actual rock failure. Therefore, the cement mortar sample is notably suitable for simulating rock damage. In addition, the specimen is relatively easy to prepare, and the tests are repeatable. Thus, cement mortar is selected as the material for our experiment.

The rock-like specimens are made of water, sand and cement with a volume ratio of 1:2:1. The dimensions (height  $\times$  width  $\times$  thickness) of the specimen are 150 mm  $\times$  150 mm  $\times$  30 mm. To create the existing joint, a mica sheet (70 mm long  $\times$  30 mm wide  $\times$  0.4 mm thick) was inserted into and remained in the specimen. The specimens were cast in a special steel mould to ensure highly flat surfaces, and the mould was removed when the mortar hardened. Then, the specimens were placed in the tank for three days, and all samples were maintained in the standard constant-temperature curing box for 28 days. During the curing process, the temperature and humidity were maintained at 25 degrees and 90%, respectively. The dip direction of the joint set is assumed to be identical to the cutting load direction [3], and the joint orientation  $\alpha$  between the tunnel axis and the joint plane varies among 0°, 30°, 60° and 90°. The distance between the position of indentation and the centre of the joint is 55 mm. The specimen details are shown in Fig. 1. The basic mechanical parameters of the materials are shown in Table 1. Table 2 provides the detailed description of the geometrical parameter values for each specimen in this study.  $S$  is the specimen,  $\sigma$  is the confining stress, and  $\alpha$  is the joint angle. For example, for S-7.5-30, the confining stress is 7.5 MPa, and the joint angle is 30°.

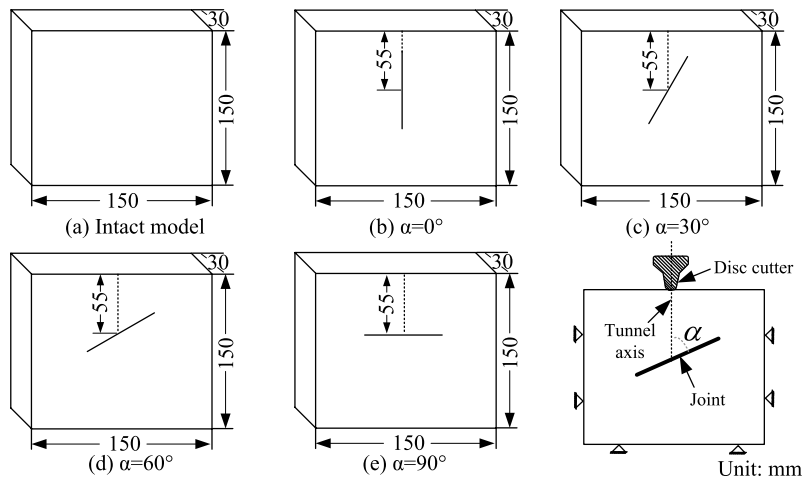


Fig. 1. Joint geometry in the specimens.

Table 2  
Parameters for each specimen.

Number	Specimen ID	$\sigma$	$\alpha$	Number	Specimen ID	$\sigma$	$\alpha$
1	S-2.5-0	2.5	0	9	S-7.5-0	7.5	0
2	S-2.5-30	2.5	30	10	S-7.5-30	7.5	30
3	S-2.5-60	2.5	60	11	S-7.5-60	7.5	60
4	S-2.5-90	2.5	90	12	S-7.5-90	7.5	90
5	S-5-0	5	0	13	S-10-0	10	0
6	S-5-30	5	30	14	S-10-30	10	30
7	S-5-60	5	60	15	S-10-60	10	60
8	S-5-90	5	90	16	S-10-90	10	90

## 2.2. Test apparatus

The test machine (model TRW-3000), as illustrated in Fig. 2, was designed by the Central South University and used for the indentation tests in this study. Liu et al. [8] previously described this triaxial test system. The testing system consists of the operation and control system, loading system, servo-controller, and rock-breaking system. Specifically, the operation and control system consists of a computer, of the supported data acquisition software, and of the force and displacement control sensors in the loading system. The loading system is independently exerted by oil pressure in two orthogonal directions  $X$  and  $Z$  with maximum vertical ( $Z$ ) and horizontal ( $X$ ) loads of 3000 and 2000 kN, respectively. The rock-breaking system consists of the half full-scale disc cutter, connecting the rod and the bearing tank. As part of an actual TBM tool, the half full-scale disc cutter was used, whose dimension is shown in Fig. 3a. The cutting edge is 6.5 mm wide, and the phase angle is 20°. The disc cutter is fixed on the impacting rod with two screws, as shown in Fig. 3(b). The impacting rod is fixed on the  $X$  direction of the oil tank.

## 2.3. Experimental procedure

As shown in Fig. 2, a series of laboratory tests was conducted on model TRW-3000. This series of test was applied in the horizontal ( $X$ ) and vertical ( $Z$ ) directions. In the experiment, the cutter was loaded with displacement control, the rate of intrusion of the cutter was approximately 0.05 mm/s in the horizontal ( $X$ ) direction, and the bearing tank was constant in the indentation process. The confining stress was supplied with force control in the vertical ( $Z$ ) direction. The confining stresses were 0, 2.5, 5, 7.5, and 10 MPa. The specimens were induced until the indentation depth was 10 mm, and the crack propagation and failure process were monitored using a video recorder.

## 3. Results and discussion

### 3.1. Effects of the confining stress on the rock-breaking process in intact rock

#### 3.1.1. Crack propagation in intact rock

Fig. 4 shows the laboratory test results of rock breaking without confining stress. The laboratory tests show three main aspects: (1) a clear long median crack propagates along the indentation direction because of the tensile stress; (2) there is

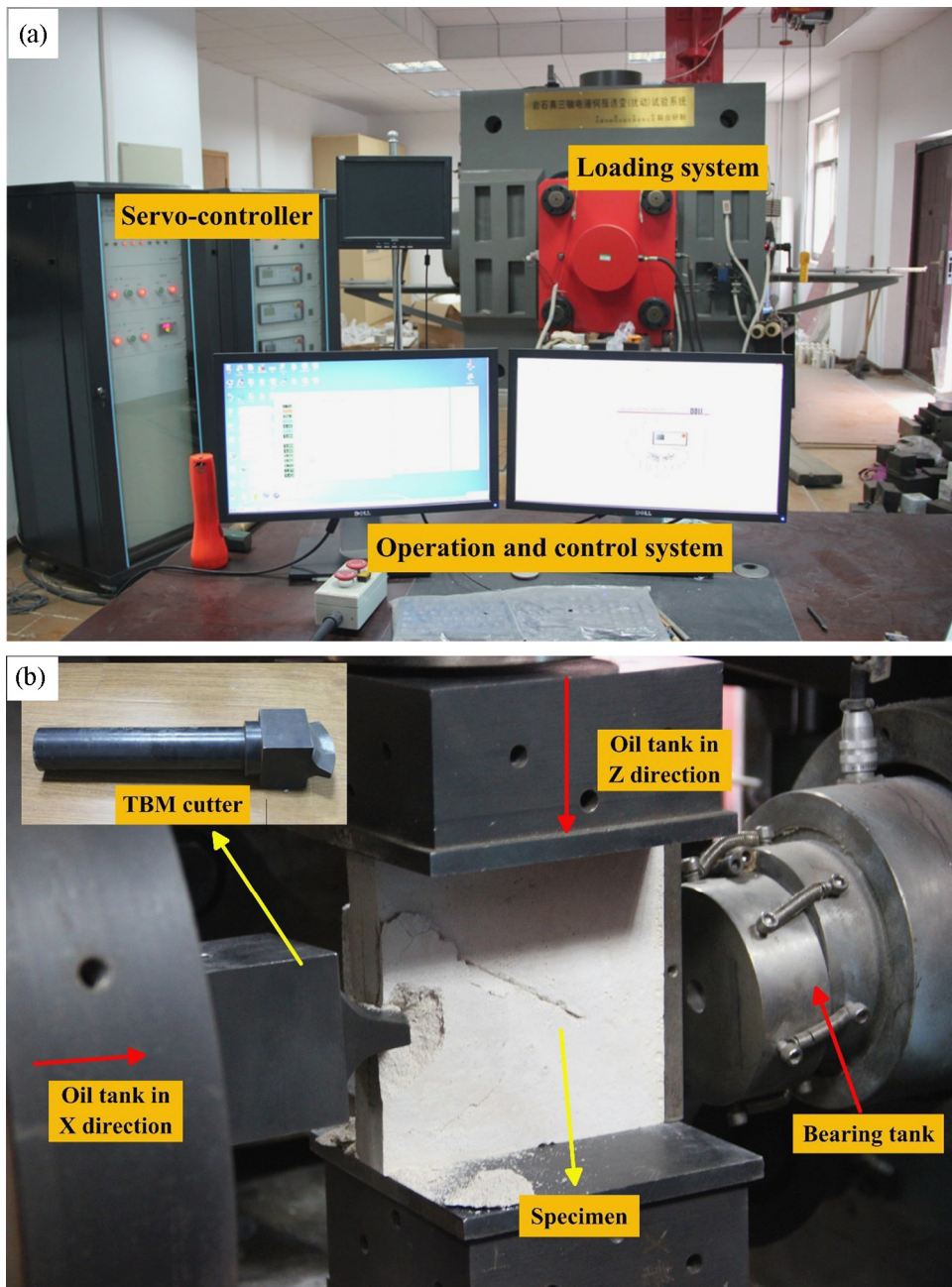


Fig. 2. Sketch of the test equipment: (a) an overview of the testing system; (b) rock-breaking system.

no obvious side crack and broken zones on both sides of the cutter; and (3) the rock-breaking process without confining stress exhibits a brittle behaviour.

Because there must be confining stress in the surrounding rock environment during TBM excavation, indentation tests without confining stress were not performed in subsequent experiments. Fig. 5a shows the typical crack propagation mode in the rock-breaking process when the confining stress was 2.5 MPa. In this experiment, a crushed zone formed under the disc cutter. Then, the median and side crack initiates beneath the crush zone. Rostami and Ozdemir [11] also obtained a similar conclusion as shown in Fig. 5b. Specifically, when the cutter acts on the specimen, a failure zone emerges immediately in front of the cutter. Because of high stress concentrations, some fine-grained crushed rock is developed immediately in front of the cutter. Further ahead is a zone of potential damage area. The crushed zone forms with increasing indentation. Then, minor cracks initiate beneath the crushed zone. The minor cracks can be divided into median cracks and side cracks. The median cracks mainly initiate immediately in front of the crushed zone and propagate along the indentation

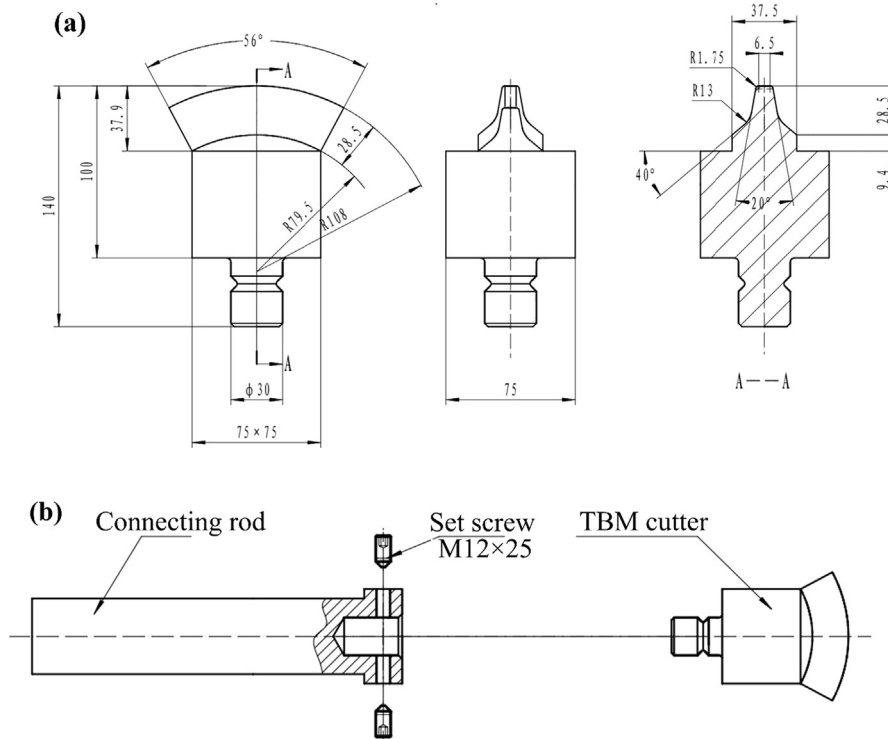


Fig. 3. Schematic diagram of the cutter: (a) geometric parameters of the cutter (unit: mm); (b) connecting the rod and the TBM cutter.



Fig. 4. Failure mode of rock breaking without confining stress.

direction; the side cracks mainly initiate from both sides of the crushed zone and propagate towards the free surface. The crack propagation process is consistent with the simulation results [5,7,13,28].

### 3.1.2. Failure modes in an intact rock

Fig. 6 shows a typical fracture characteristic of the specimen in the indentation tests. The abrasive area is directly under the crushed zone, and the fracture surface is relatively rough, as shown in Fig. 6a. This damage zone is mainly formed by the median crack, which is driven by the tensile stress. For the side crack, the fracture face is smooth (Fig. 6b), which



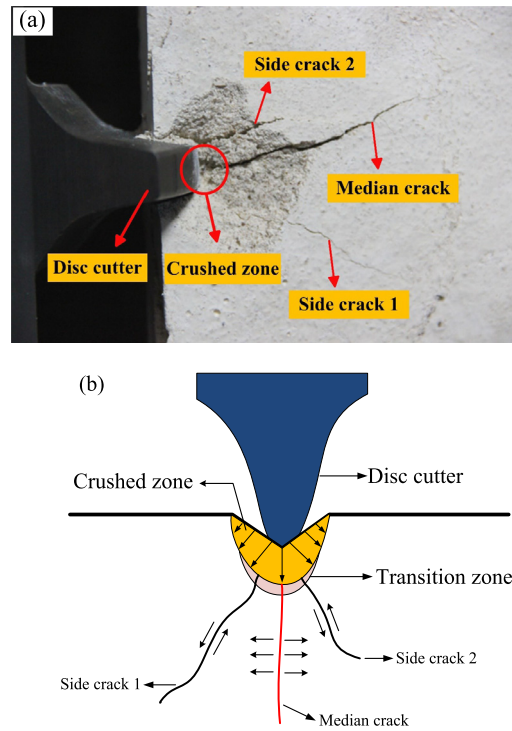


Fig. 5. Typical crack propagation mode in the specimen: (a) photograph of the typical crack patterns; (b) crack propagation mode for the rock mass [11].

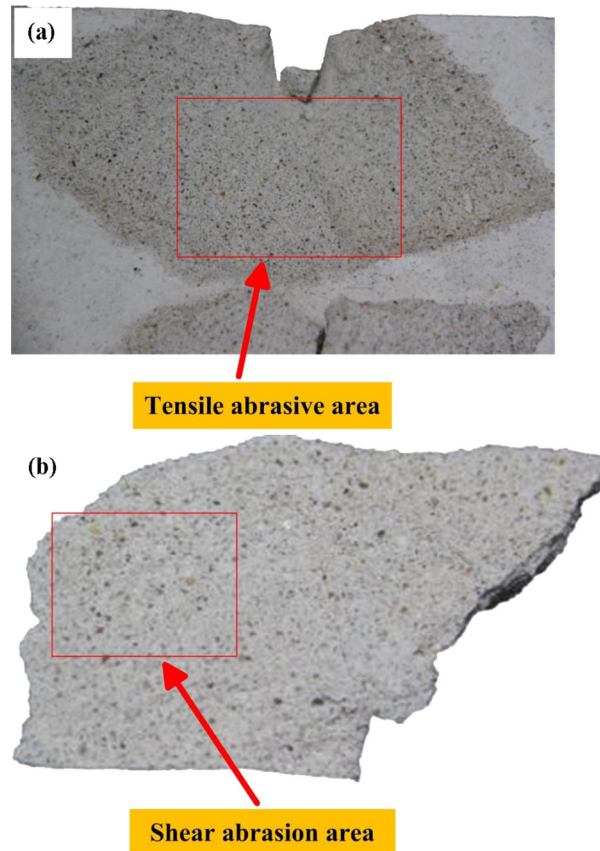


Fig. 6. Typical fracture character of the specimen, (a) tensile abrasive area; (b) shear abrasive area.

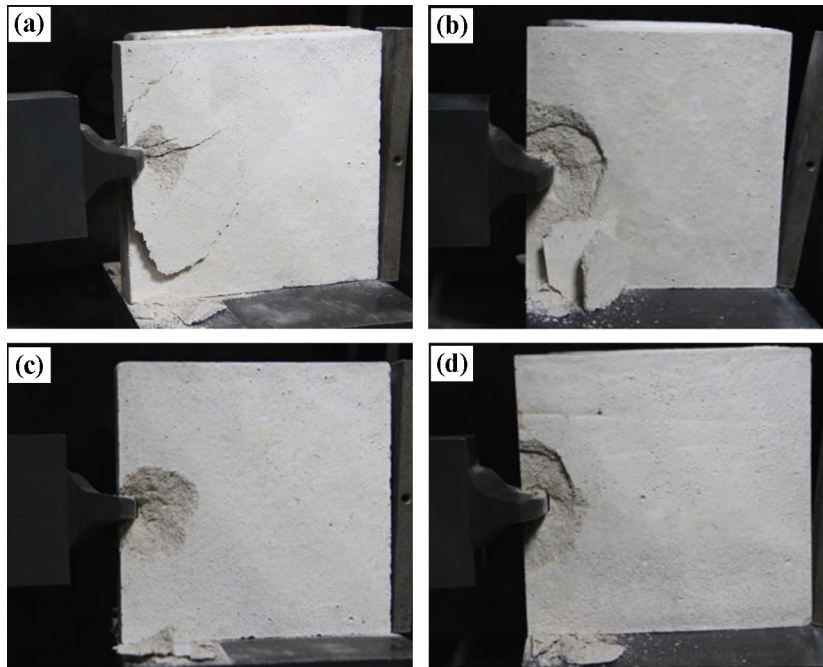


Fig. 7. Illustration of the sample's failure with different confining stresses: (a) 2.5 MPa, (b) 5 MPa, (c) 7.5 MPa, (d) 10 MPa.

indicates that the early crack propagation is mainly driven by the shear stress, and the later rock-breaking process is mainly driven by the tensile stress.

Previous studies have proven that the confining stress is a significant factor that affects the rock fragmentation efficiency. In this section, four additional laboratory tests on rock-like specimens with different confining stresses (2.5, 5, 7.5 and 10 MPa) were performed, and the effect of the confining stress on the crack propagation and failure modes was further analysed.

The final rock fragmentation patterns for specimens with four different confining stress values of 2.5, 5, 7.5, and 10 MPa are shown in Fig. 7. When the confining stress is 2.5 MPa, the median crack is well developed, and the major breakage is mainly caused by tensile cracks that propagate along the indentation direction, as shown in Fig. 7a. With the increase in confining stress, the propagation of the median crack is limited, and the main failure depth is reduced. When the confining stress increases to 10 MPa, no median crack appears, whereas more side cracks propagate from the two sides of the crushed zone to the free surface; then, chips are formed at the free surface. In other words, the median crack is more likely generated immediately in front of the crushed zone when the confining stress is low. Under high confining stress, more lateral cracks initiate at the crushed zone and propagate towards the free surface, which results in rock chips at the free surface.

### 3.1.3. Indentation force in intact rock

The indentation force and indentation depth curves for four different confining stresses of 2.5, 5, 7.5, and 10 MPa are shown in Fig. 8. The indentation force is the resistance of the specimens during the cutter's indentation, and the indentation depth is the depth of the cutter's intrusion into the specimens. As shown in Fig. 8, when the confining pressure is 2.5, 5, 7.5, and 10 MPa, the peak indentation force is 15.99, 17.49, 19.36, and 21.08 kN, respectively. The peak indentation force increases with the increase in confining stress during the indentation process, i.e. a high thrust force is required when the TBM cutter operates in high-confining-stress conditions. This conclusion appears to be similar to those of previous simulation studies [29].

## 3.2. Effects of the joint orientation on the rock-breaking process in jointed rock

### 3.2.1. Failure modes in jointed rock

Fig. 9 shows the crack propagation and failure modes of rock breaking under the disc cutter when the joint angle is  $0^\circ$  and the confining stress varies from 2.5, 5, 7.5 to 10 MPa. Fig. 9 shows that the medium cracks initiate from the crushed zone and gradually propagate along the jointed plane. Meanwhile, two cracks initiate at the upper tips of the jointed plane and propagate towards the free surface. With further increase in the indentation depth, the cracks coalesce with the side cracks and finally form rock chips.

As shown in Figs. 10 and 11, when the confining stress is low, the cracks propagate along certain directions; medium and side cracks initiate and propagate from the crushed zone and terminate at the joint plane. Meanwhile, some cracks

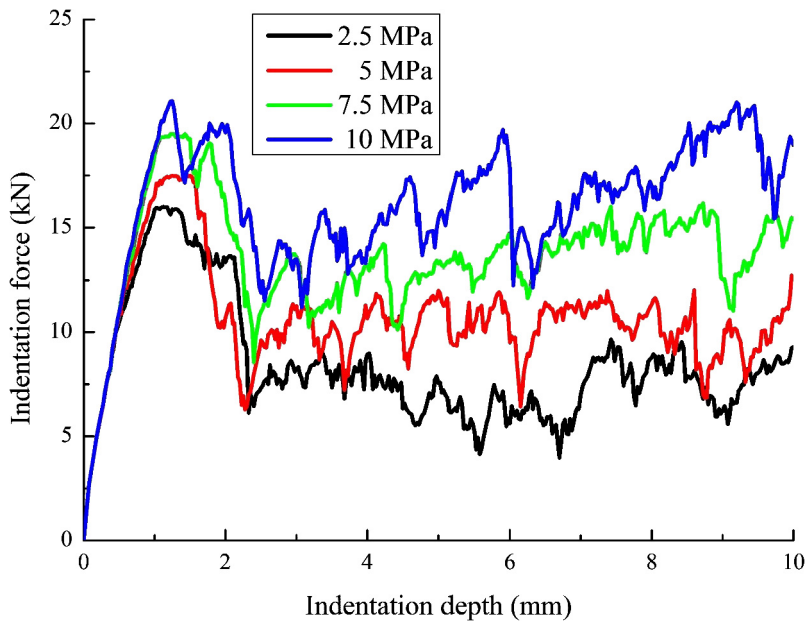


Fig. 8. Force-indentation curve with different confining stresses: (a) 2.5 MPa, (b) 5 MPa, (c) 7.5 MPa, (d) 10 MPa.

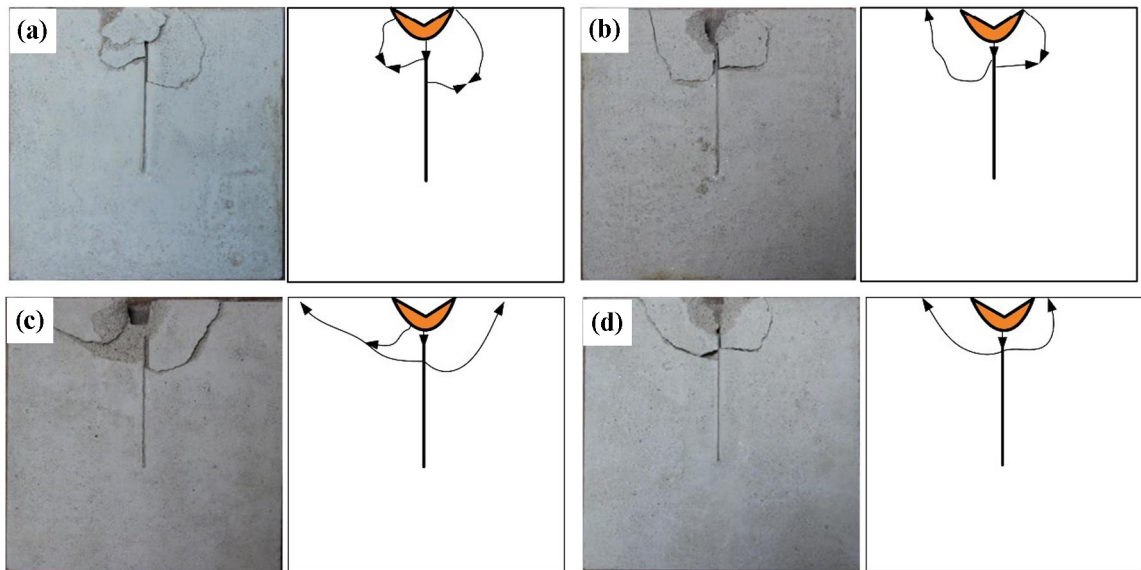


Fig. 9. Effect of the confining stress on the final failure modes ( $\alpha = 0^\circ$ ): (a) S-2.5-0, (b) S-5-0, (c) S-7.5-0, (d) S-10-0.

initiate from the joint plane and propagate upward to the free surface. When those cracks coalesce with the median and side cracks, the rock chips are formed. However, when the confining stress increases to 7.5 and 10 MPa, the initiation and propagation of the median crack are restrained, as shown in Figs. 10c and 10d. Compared with Fig. 6, the jointed specimen has final failure modes similar to those of the intact specimen, i.e. the existence of joints has no obvious effect on the failure mode when the confining stress increases to a certain value.

When the joint angle  $\alpha$  increases to  $90^\circ$ , the median crack is initiated immediately in front of the crushed zone, propagates along the induce way, and finally terminate at the joint surface. The side cracks initiate immediately in front of the crushed zone and propagate symmetrically, as shown in Figs. 12a and b.

The above analysis shows that the joint plane significantly affects the rock failure modes when the confining stress is low. However, when the confining stress increases to a certain value, the presence of the joints has no effect on the failure mode of the specimens. The failure modes of rock breaking at low confining stress can be classified as follows: (1) when the joint angle is  $0^\circ$ , the crack initiates at the upper tips of the jointed plane and coalesces with the side crack; then, rock chips are formed. (2) When the joint angle is  $30^\circ$  and  $60^\circ$ , the crack initiates under the crushed zone and propagates downward



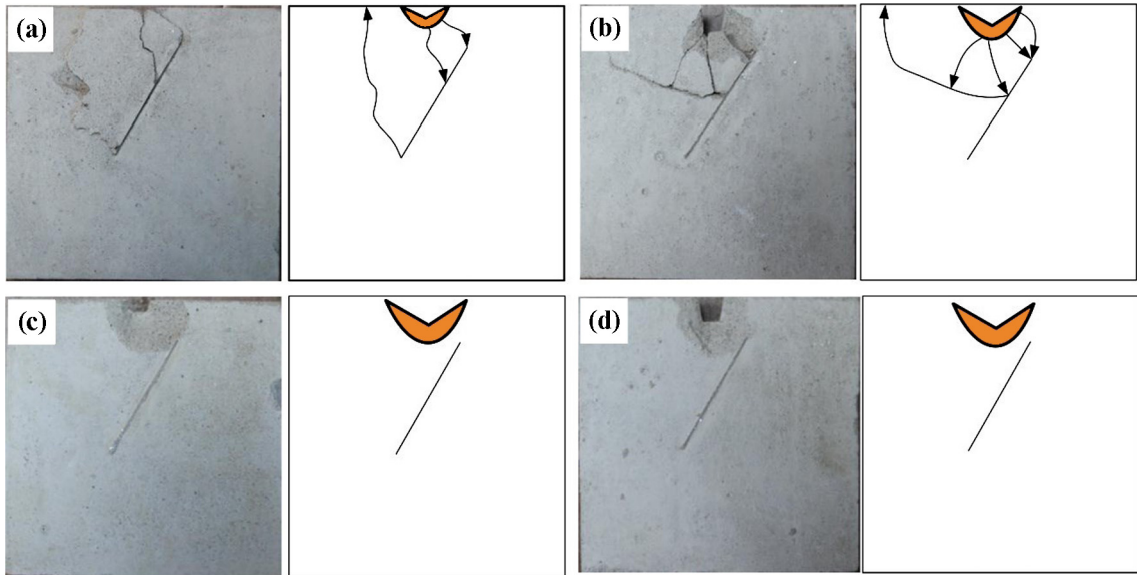


**Fig. 10.** Effect of the confining stress on the final failure modes ( $\alpha = 30^\circ$ ): (a) S-2.5-30, (b) S-5-30, (c) S-7.5-30, (d) S-10-30.

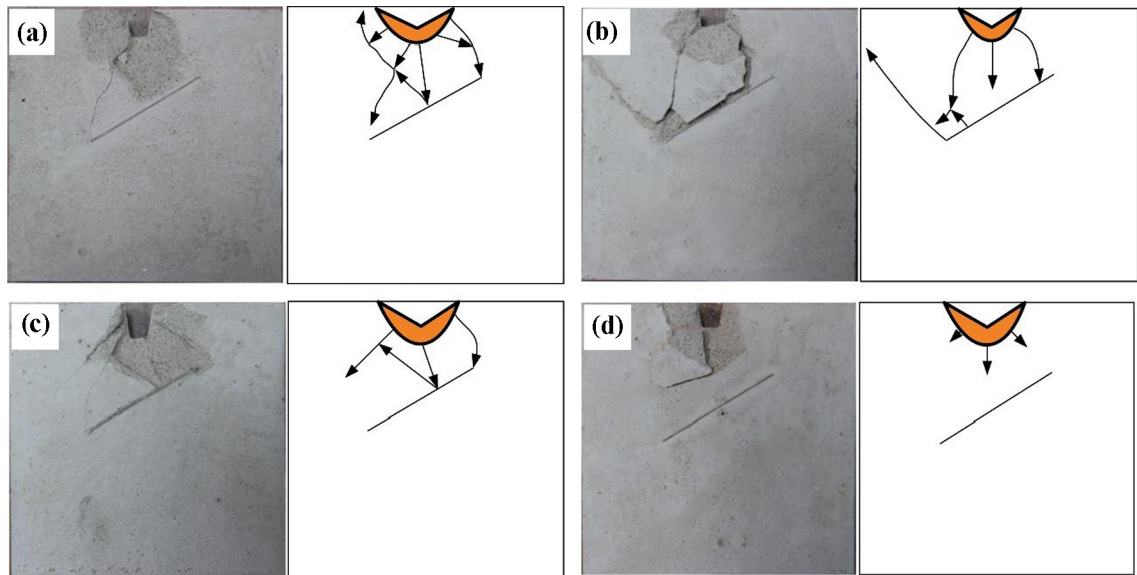


**Fig. 11.** Effect of the confining stress on the final failure modes ( $\alpha = 60^\circ$ ): (a) S-2.5-60, (b) S-5-60, (c) S-7.5-60, (d) S-10-60.

the joint plane; then, rock chips are formed. (3) When the joint angle is  $30^\circ$  and  $60^\circ$ , the crack initiates at the joint plane and propagates upward the free surface; then, rock chips are formed. (4) When the joint angle is  $90^\circ$ , the crack initiates from the crushed zone, propagates towards the joint plane, and finally terminates at the joint plane; then, rock chips are formed.

### 3.2.2. Indentation force in jointed rock

The change in peak indentation force with different joint orientations and confining stresses is shown in Fig. 13, where the peak indentation force increases with the increase in confining stress. Moreover, the intact specimens have a larger peak indentation force than the jointed rock-like specimens. In particular, when the confining stress is 2.5 MPa, the peak indentation force is significantly different, which indicates that the joint orientation considerably affects the peak indentation force when the confining stress is low. Specifically, when the joint orientation is  $30^\circ$  and  $60^\circ$ , the peak indentation force is lower than that of the other specimens. The experimental results of the final failure modes also prove that the joint orientation has a considerable effect on the rock-breaking process when the confining stress is low. However, there is no obvious difference when the confining stress increases to 10 MPa.

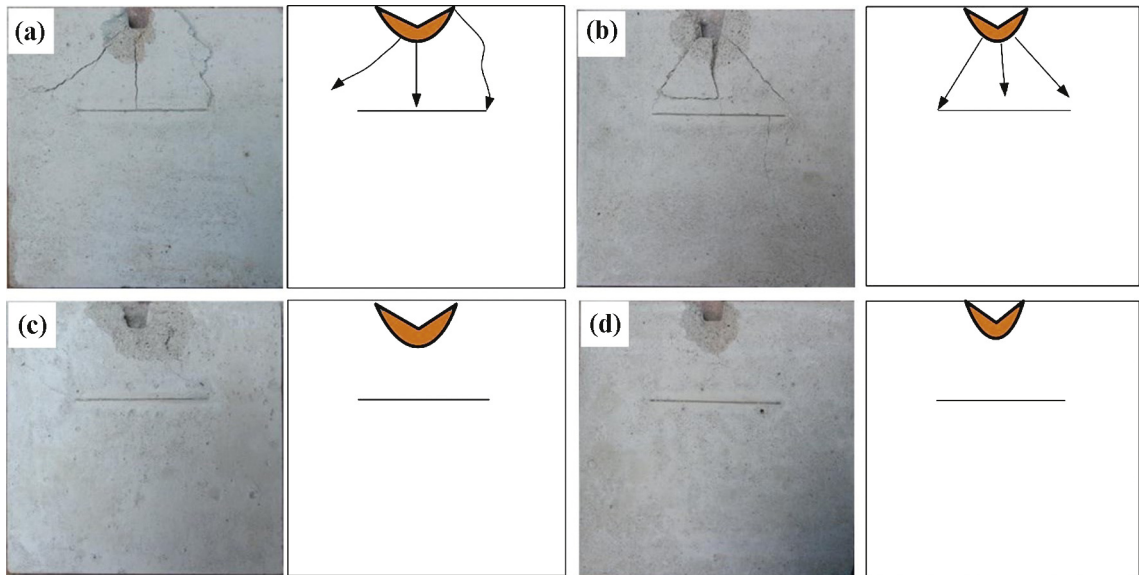


Fig. 12. Effect of the confining stress on the final failure modes ( $\alpha = 90^\circ$ ): (a) S-2.5-90, (b) S-5-90, (c) S-7.5-90, (d) S-10-90.

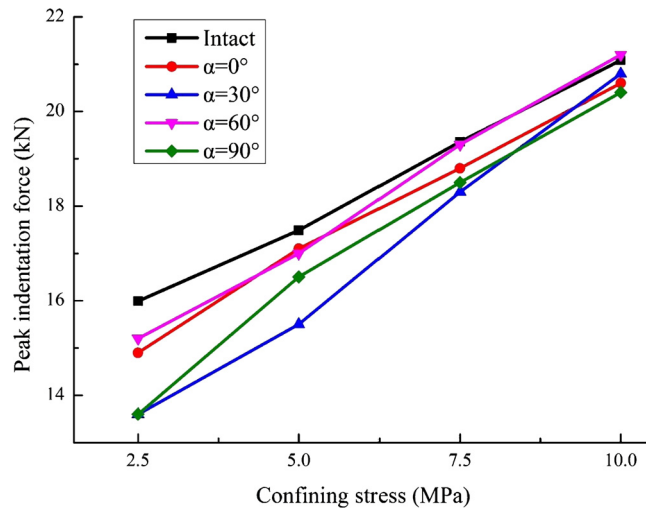


Fig. 13. Peak indentation force of rock-like specimens with different confining stresses and joint orientations.

The above analysis indicates that when the confining stress is not notably high, and the rock mass with a certain joint angle is more easily broken. In addition, the peak indentation force increases with the increase in confining stress, which indicates that the TBM cutter requires a high thrust force in a high-confining-stress condition.

#### 4. Conclusions

In this paper, a series of laboratory tests was performed to investigate the crack propagation and failure modes of intact and jointed rocks under different confining stresses. The laboratory test results for the intact and jointed rocks under different confining stresses are consistent with previous results of other scholars. Moreover, the crack propagation and failure modes in a jointed rock mass under different confining stresses are revealed. These results improve the understanding of jointed rock breaking induced by the TBM cutter under confining stress. The main conclusions are as follows.

(1) Peak indentation force increases with the increase in confining stress during the indentation process. The median crack is well developed at low confining stress. However, the median crack is restrained, and the rock chip formation is mainly caused by side crack propagation when the confining stress increases.

(2) The failure mode is affected by the joint orientation at low confining stress. The failure modes can be summarised as follows: when the joint angle is  $0^\circ$ , the crack initiates at the upper tips of the jointed plane and coalesces with the side crack; then, rock chips are formed. When the joint angle is  $30^\circ$  or  $60^\circ$ , the crack initiates under the crushed zone and

propagates downward in the joint plane; then, rock chips are formed. When the joint angle is  $30^\circ$  or  $60^\circ$ , the crack initiates at the joint plane and propagates upward the free surface; then, rock chips are formed. When the joint angle is  $90^\circ$ , the crack initiates from the crushed zone, propagates towards the joint plane, and terminates at the joint plane; finally, rock chips are formed.

## Acknowledgements

This research was supported by the National Natural Science Foundation of China (grant numbers 51174228, 11772358), the National Basic Research Program of China (grant number 2013CB035401), and the Fundamental Research Funds for the Central Universities, China (grant number 2018zzts211). The authors are grateful for this support. The authors are also very grateful to the anonymous reviewers for their valuable comments that have significantly improved the paper.

## References

- [1] Q.M. Gong, L.J. Yin, H.S. Ma, J. Zhao, TBM tunnelling under adverse geological conditions: an overview, *Tunn. Undergr. Space Technol.* 57 (2016) 4–17.
- [2] N. Barton, *TBM Tunnelling in Jointed and Faulted Rock*, A.A. Balkema, Rotterdam, The Netherlands, 2000.
- [3] Q.M. Gong, J. Zhao, Y.Y. Jiao, Numerical modelling of the effects of joint orientation on rock fragmentation by TBM cutters, *Tunn. Undergr. Space Technol.* 20 (2) (2005) 183–191.
- [4] M. Jiang, Y. Liao, H. Wang, Y. Sun, Distinct element method analysis of jointed rock fragmentation induced by TBM cutting, *Eur. J. Environ. Civ. Eng.* 7 (2017) 1–20.
- [5] S.F. Zhai, X.P. Zhou, J. Bi, N. Xiao, The effects of joints on rock fragmentation by TBM cutters using general particle dynamics, *Tunn. Undergr. Space Technol.* 57 (2016) 162–172.
- [6] N. Innurato, C. Oggeri, P.P. Oreste, R. Vinai, Experimental and numerical studies on rock breaking with TBM tools under high stress confinement, *Rock Mech. Rock Eng.* 40 (5) (2007) 429–451.
- [7] H.S. Ma, L.J. Yin, H.G. Ji, Numerical study of the effect of confining stress on rock fragmentation by TBM cutters, *Int. J. Rock Mech. Min. Sci.* 48 (6) (2011) 1021–1033.
- [8] J. Liu, P. Cao, D.Y. Han, Sequential indentation tests to investigate the influence of confining stress on rock breakage by tunnel boring machine cutter in a biaxial state, *Rock Mech. Rock Eng.* 49 (4) (2015) 1479–1495.
- [9] X.F. Li, S.B. Wang, S.R. Ge, R. Malekian, Z.X. Li, Numerical simulation of rock fragmentation during cutting by conical picks under confining pressure, *C. R. Mecanique* 345 (12) (2017) 890–902.
- [10] Y.C. Pan, Q.S. Liu, J.P. Liu, X.X. Peng, X.X. Kong, Full-scale linear cutting tests in Chongqing sandstone to study the influence of confining stress on rock cutting forces by TBM disc cutter, *Rock Mech. Rock Eng.* 2 (2018) 1–17.
- [11] J. Rostami, L. Ozdemir, New model for performance prediction of hard rock TBMs, in: *Rapid Excavation and Tunnelling Conferences*, Boston, MA, USA, 1993.
- [12] A. Bruland, *Hard Rock Tunnel Boring*, PhD thesis, Norwegian University of Science and Technology, Trondheim, Norway, 1998.
- [13] H.Y. Liu, S.Q. Kou, P.A. Lindqvist, C.A. Tang, Numerical simulation of the rock fragmentation process induced by indenters, *Int. J. Rock Mech. Min. Sci.* 39 (4) (2002) 491–505.
- [14] M.F. Marji, H.H. Nasab, A.H. Morshedi, Numerical modeling of crack propagation in rocks under TBM disc cutters, *J. Mech. Mater. Struct.* 4 (3) (2009) 605–627.
- [15] M.F. Marji, Simulation of crack coalescence mechanism underneath single and double disc cutters by higher order displacement discontinuity method, *J. Cent. South Univ. Technol.* 22 (3) (2015) 1045–1054.
- [16] L.J. Yin, Q.M. Gong, H.S. Ma, J. Zhao, X.B. Zhao, Use of indentation tests to study the influence of confining stress on rock fragmentation by a TBM cutter, *Int. J. Rock Mech. Min. Sci.* 72 (2014) 261–276.
- [17] L.J. Yin, Q.M. Gong, J. Zhao, Study on rock mass boreability by TBM penetration test under different in situ stress conditions, *Tunn. Undergr. Space Technol.* 43 (7) (2014) 413–425.
- [18] J. Liu, J. Wang, The effect of indentation sequence on rock breakages: a study based on laboratory and numerical tests, *C. R. Mecanique* 346 (1) (2018) 26–38.
- [19] M. Entacher, S. Lorenz, R. Galler, Tunnel boring machine performance prediction with scaled rock cutting tests, *Int. J. Rock Mech. Min. Sci.* 70 (9) (2014) 450–459.
- [20] L.H. Chen, J.F. Labuz, Indentation of rock by wedge-shaped tools, *Int. J. Rock Mech. Min. Sci.* 43 (7) (2006) 1023–1033.
- [21] D.F. Howarth, The effect of jointed and fissured rock on the performance of tunnel boring machines, in: *Proceedings of the International Symposium on Weak Rock*, Tokyo, Japan, September 1981.
- [22] H. Yang, J. Liu, B. Liu, Investigation on the cracking character of jointed rock mass beneath TBM disc cutter, *Rock Mech. Rock Eng.* 5 (2018) 1–15.
- [23] F. Zou, H.B. Li, Q.C. Zhou, Z.Z. Mo, X.M. Zhu, L. Niu, Experimental study of influence of joint space and joint angle on rock fragmentation by TBM disc cutter, *Rock Soil Mech.* 33 (6) (2012) 1640–1646.
- [24] H.S. Ma, L.J. Yin, Q.M. Gong, J. Wang, Experimental study on the effect of joint spacing on fragmentation modes and penetration rate under TBM disc cutters, *Appl. Mech. Mater.* 353–356 (1) (2011) 890–894.
- [25] K.H. Li, P. Cao, J. Liu, Experimental study of effects of joint on rock fragmentation mechanism by TBM cutters, *Appl. Mech. Mater.* 711 (2014) 44–47.
- [26] P. Cao, Q.B. Lin, K.H. Li, D.Y. Han, Effects of joint angle and joint space on rock fragmentation efficiency by two TBM disc cutters, *J. Cent. South Univ. Technol.* 48 (5) (2017) 1293–1299.
- [27] Q.B. Lin, P. Cao, K.H. Li, R.H. Cao, K.P. Zhou, H.W. Deng, Experimental study on acoustic emission characteristics of jointed rock mass by double disc cutter, *J. Cent. South Univ. Technol.* 25 (2) (2018) 357–367.
- [28] X.P. Zhang, P.Q. Ji, Q.S. Liu, Q. Liu, Q. Zhang, Z.H. Peng, Physical and numerical studies of rock fragmentation subject to wedge cutter indentation in the mixed ground, *Tunn. Undergr. Space Technol.* 71 (2018) 354–365.
- [29] Q.S. Liu, Y.L. Jiang, Z.J. Wu, X.Y. Xu, Q. Liu, Investigation of the rock fragmentation process by a single TBM cutter using a Voronoi element-based numerical manifold method, *Rock Mech. Rock Eng.* 4 (2017) 1–16.